

Anisotropy of the magnetoviscous effect in ferrofluids

Patrick Ilg,^{1,*} Martin Kröger,² and Siegfried Hess¹

¹*Institut für Theoretische Physik, Technische Universität Berlin, Hardenbergstr. 36, D-10623 Berlin, Germany*

²*Polymer Physics, ETH Zürich, Wolfgang-Pauli-Str. 10, CH-8093 Zürich, Switzerland*

(Received 9 December 2004; published 26 May 2005)

The anisotropy of the magnetoviscous effect in ferrofluids subjected to weak planar Couette flow is investigated by extensive molecular simulations. The field and concentration dependence of the viscosity coefficients are found to depend on the relative orientation of the magnetic field with respect to the flow geometry. Comparison with dynamical mean-field models shows satisfactory agreement for moderate interaction strengths. In the semidilute regime it is found that the anisotropy contains valuable information on particle interaction.

DOI: 10.1103/PhysRevE.71.051201

PACS number(s): 75.50.Mm, 83.80.Hj, 83.80.Gv, 47.32.-y

I. INTRODUCTION

Magnetic fluids have attracted considerable interest since their viscous properties can be manipulated by external magnetic fields [1,2]. Here, we study the anisotropy of the magnetoviscous effect (MVE), i.e., the dependence of the viscosity not only on the magnitude of the magnetic field but also on its relative orientation to the flow geometry.

It has been known since the first experimental observation of the magnetoviscous effect by McTague [3] that the magnetoviscous effect is anisotropic, i.e., the viscosity changes in a different way depending on the relative orientation of the magnetic field and the velocity gradients. A pipe flow geometry with the magnetic field oriented either in flow or perpendicular to the flow direction was employed in the experiment of McTague. Early theoretical explanation by Shliomis [4] of the magnetoviscous effect successfully accounts for the different values of viscosity observed in these experiments. On the other hand, the model [4] fails to account for the anisotropy of the MVE observed in a parallel plate geometry [5]. In this experiment, three different viscosity coefficients are measured for the magnetic field oriented in the flow, gradient, and vorticity direction, respectively. More refined theoretical models like the chain model [6] or the dynamical mean-field model [7] are able to describe these results at least qualitatively. Subsequent experimental investigations have revealed other shortcomings of the model [4] like concentration dependence of the viscosity, normal stress differences, and off-equilibrium magnetization in an elongational flow (see, e.g. [8], Odenbach in [1] and references therein). Unfortunately, these studies have focused on a fixed orientation of the magnetic field and therefore cannot give direct information on the anisotropy of the MVE.

In this paper, we present extensive molecular simulations on the anisotropy of the MVE in weak planar Couette flow and its dependence on the magnetic field, concentration, and interaction strength. This paper is organized as follows. In Sec. II the model system is presented and the relevant macroscopic quantities are given. Section III reviews the simpli-

fied non-interacting model [4] and dynamical mean-field model [7]. Simulation results of the model system are reported in Sec. IV together with a comparison to the simplified models. Finally, some conclusions are offered in Sec. V.

II. MODEL EQUATIONS

We study the same model that was already employed in previous studies [9,10]. In this model, N identical spherical particles of diameter σ are considered. Each particle carries an embedded magnetic point dipole of strength m . The position of particle j and the orientation of its magnetic moment are denoted by \mathbf{r}_j and \mathbf{u}_j , respectively. Let \mathbf{H} denote the uniform internal magnetic field of strength H . The interaction energy of particle j with the magnetic field $\Phi_j^H = \Phi^H(\mathbf{u}_j)$, the interaction energy of particles j and k due to dipolar interactions $\Phi_{jk}^{\text{dd}} = \Phi^{\text{dd}}(\mathbf{r}_{jk}, \mathbf{u}_j, \mathbf{u}_k)$ and steric interactions $\Phi_{jk}^s = \Phi^s(r_{jk})$ are given by

$$\Phi^H(\mathbf{u}) = -k_B T h \mathbf{u} \cdot \mathbf{H} / H, \quad (1)$$

$$\Phi^{\text{dd}}(\mathbf{r}, \mathbf{u}, \mathbf{u}') = k_B T \lambda \frac{\sigma^3}{r^3} [\mathbf{u} \cdot \mathbf{u}' - 3(\mathbf{u} \cdot \hat{\mathbf{r}})(\mathbf{u}' \cdot \hat{\mathbf{r}})], \quad (2)$$

$$\Phi^s(r) = \begin{cases} 4\epsilon [C(r) - C(r_{\text{cut}})] & \text{for } r \leq r_{\text{cut}}, \\ 0 & \text{elsewhere,} \end{cases} \quad (3)$$

where $\mathbf{r}_{jk} = \mathbf{r}_j - \mathbf{r}_k$ is the connector vector between particles j and k , $\hat{\mathbf{r}}_{jk} = \mathbf{r}_{jk} / r_{jk}$ with r_{jk} the distance between the particles. In Eqs. (1) and (2), we have introduced the Langevin parameter $h = \mu_0 m H / k_B T$ and the dimensionless dipolar interaction parameter

$$\lambda = \frac{\mu_0 m^2}{4\pi\sigma^3 k_B T}. \quad (4)$$

Boltzmann's constant and absolute temperature are denoted by k_B and T , respectively. Following [9,10], we choose the WCA potential for the steric interaction, i.e., $C(r) = (\sigma/r)^{12} - (\sigma/r)^6$ and $r_{\text{cut}} = 2^{1/6}\sigma$, i.e., a purely repulsive potential with smooth cutoff at $r = r_{\text{cut}}$. Same as in [9,10], we assume that the system under study is surrounded by a uniform medium

*Corresponding author. Email address: ilg@physik.tu-berlin.de

with infinite magnetic permeability. In this case, metallic boundary conditions apply and the internal magnetic field \mathbf{H} coincides with the applied external field.

A. Translational and orientational dynamics

If M and Θ denote the mass and the moment of inertia tensor of the ferromagnetic particles, the equations of motion for the translational and orientational dynamics read [9–12]

$$M\dot{\mathbf{v}}_j = \sum_{k=1}^N \mathbf{F}_{jk} - \zeta_t[\mathbf{v}_j - \mathbf{v}(\mathbf{r}_j)] + \mathbf{F}_j^{\mathbf{B}}, \quad (5)$$

$$\Theta \cdot \dot{\boldsymbol{\omega}}_j = m \mathbf{u}_j \times \mathbf{H} + \sum_{k=1}^N \mathbf{N}_{jk}^{\text{dd}} - \zeta_{\text{rot}}[\boldsymbol{\omega}_j - \boldsymbol{\Omega}(\mathbf{r}_j)] + \mathbf{N}_j^{\mathbf{B}}, \quad (6)$$

where $\mathbf{v}_j = \dot{\mathbf{r}}_j$ and $\boldsymbol{\omega}_j = \mathbf{u}_j \times \dot{\mathbf{u}}_j$ denote the translational and angular velocity of particle j , respectively. The forces \mathbf{F}_{jk} and torques $\mathbf{N}_{jk}^{\text{dd}}$ are obtained from the interaction potential by

$$\mathbf{F}_{jk} = -\partial\Phi_{jk}/\partial\mathbf{r}_{jk}, \quad \mathbf{N}_{jk}^{\text{dd}} = -\mathcal{L}_j\Phi_{jk} \quad (7)$$

(no summation convention), where $\Phi_{jk} = \Phi_{jk}^{\text{dd}} + \Phi_{jk}^{\text{s}}$ is the total interaction potential of particles j and k and $\mathcal{L}_j \equiv \mathbf{u}_j \times \partial/\partial\mathbf{u}_j$ is the rotational operator. The first term on the right-hand side of Eq. (6) equals $-\mathcal{L}_j\Phi_j^{\text{H}}$, which is the torque exerted by the magnetic field. Primes on summation symbols imply that the term $j=k$ should be omitted from the sums. The effect of the solvent is modeled by Brownian forces $\mathbf{F}_j^{\mathbf{B}}$ and torques $\mathbf{N}_j^{\mathbf{B}}$ with $\langle \mathbf{F}_j^{\mathbf{B}} \rangle = \langle \mathbf{N}_j^{\mathbf{B}} \rangle = \mathbf{0}$ and $\langle \mathbf{F}_j^{\mathbf{B}} \mathbf{F}_k^{\mathbf{B}} \rangle = 2k_{\text{B}}T\zeta_t\delta_{jk}\mathbf{1}$ and $\langle \mathbf{N}_j^{\mathbf{B}} \mathbf{N}_k^{\mathbf{B}} \rangle = 2k_{\text{B}}T\zeta_{\text{rot}}\delta_{jk}\mathbf{1}$. The translational ζ_t and rotational ζ_{rot} friction coefficients have been introduced. For a sphere of diameter σ in a solvent with viscosity η_s , these coefficients are given by $\zeta_t = 3\pi\eta_s\sigma$ and $\zeta_{\text{rot}} = \pi\eta_s\sigma^3$, respectively. Since hydrodynamic interactions are not included in Eqs. (5) and (6), we here consider the so-called “free-draining limit.”

B. Magnetization and viscosity coefficients

Macroscopic quantities like the magnetization and viscosity coefficients are obtained as ensemble averages. The macroscopic magnetization is defined by $\mathbf{M} = M_{\text{sat}}\bar{\mathbf{u}}$, where $M_{\text{sat}} = nm$ is the saturation magnetization with $n = N/V$ the number density of magnetic particles. The average orientation of the magnetic dipoles is calculated from $\bar{\mathbf{u}} = (1/N)\sum_{j=1}^N \mathbf{u}_j$.

In order to define the viscosity coefficients, consider the momentum balance equation of the fluid, $\rho\dot{\mathbf{v}} = -\nabla \cdot \mathbf{P} + \mathbf{f}_{\text{M}}$, where \mathbf{f}_{M} denotes the magnetic force density. The mass density and the velocity of the fluid are denoted by ρ and \mathbf{v} , respectively. Like any second rank tensor, the viscous pressure tensor \mathbf{P} can be decomposed uniquely into its isotropic, symmetric traceless, and antisymmetric part [13],

$$\mathbf{P} = p\mathbf{1} + \bar{\mathbf{P}} + \frac{1}{2}\boldsymbol{\epsilon} \cdot \mathbf{p}^{\text{a}}, \quad (8)$$

The symbol $\bar{\cdot}$ denotes the symmetric traceless part of a tensor. The antisymmetric part involves the pseudovector $\mathbf{p}^{\text{a}} = -\boldsymbol{\epsilon} \cdot \mathbf{P}$, where we have introduced the total antisymmetric tensor of rank three (Levi-Civita) is denoted by $\boldsymbol{\epsilon}$, i.e., $\boldsymbol{\epsilon} \cdot (\mathbf{a}\mathbf{b}) = \mathbf{a} \times \mathbf{b}$ for the dyadic $\mathbf{a}\mathbf{b}$ constructed by arbitrary vectors \mathbf{a} and \mathbf{b} . The isotropic pressure p is irrelevant for subsequent studies. The symmetric traceless part of the viscous stress tensor is given by [12]

$$\bar{\mathbf{P}} = -\eta_s\mathbf{D} + \frac{1}{2V}\sum_{j,k}^N \overline{\mathbf{r}_{jk}\mathbf{F}_{jk}}, \quad (9)$$

with the symmetric velocity gradient $\mathbf{D} \equiv \frac{1}{2}[\nabla\mathbf{v} + (\nabla\mathbf{v})^T]$. The antisymmetric part of the viscous pressure tensor is given by

$$\mathbf{p}^{\text{a}} = \mathbf{M} \times \mathbf{H}. \quad (10)$$

The magnetic force density \mathbf{f}_{M} can be derived from Maxwell’s magnetic pressure tensor \mathbf{P}_{M} by $\mathbf{f}_{\text{M}} = -\nabla \cdot \mathbf{P}_{\text{M}}$. If a term proportional to M^2 is adsorbed in the scalar pressure p [14], the magnetic pressure tensor can be written as $\mathbf{P}_{\text{M}} = -\mathbf{B}\mathbf{H} + (\mu_0 H^2/2)\mathbf{1}$. The magnetic induction \mathbf{B} is given by $\mathbf{B} = \mu_0(\mathbf{H} + \mathbf{M})$. The total pressure tensor $\mathbf{P} + \mathbf{P}_{\text{M}}$ is symmetric due to conservation of total angular momentum.

In a plane shear flow, $\mathbf{v} = (\dot{\gamma}y, 0, 0)$, the shear viscosity is defined by $\eta_{yx} = -P_{yx}/\dot{\gamma}$. Note, that no contribution of the Maxwell pressure tensor to the shear stress arises because of the boundary conditions for the magnetic fields \mathbf{H} and \mathbf{B} (see, e.g., Chap. 8.12 of [2]). Similar to the Miesowicz viscosities of liquid crystals [13,15,16], different viscosity coefficients η_i can be defined if the magnetic field is oriented in flow ($i=1$), in gradient ($i=2$), or in the vorticity direction ($i=3$) of the flow. In addition, a fourth viscosity coefficient is needed to fully characterize the viscous behavior. This coefficient can be chosen as η_4 , the viscosity η_{yx} that is measured if the magnetic field is oriented along the bisector of the flow and gradient direction.

Next, we consider a simplified mean-field model that allows analytical predictions of the nonequilibrium magnetization and viscosity coefficients. These predictions will later be compared to simulation results of the model just presented.

III. DYNAMICAL MEAN-FIELD MODEL

In Ref. [7], a mean-field approximation to the dynamics of the interacting many-particle system, cf. Sec. II, was proposed that extends the model of noninteracting magnetic dipoles [4] to the weakly interacting regime. The range of validity of this dynamical mean-field model was investigated in [9] for the special case, where the magnetic field is oriented in the gradient direction of the flow.

Here, we briefly summarize the dynamical mean-field model introduced in [7]. On time scales that are long enough so that the inertia term $\Theta \cdot \boldsymbol{\omega}$ can be neglected, the Langevin dynamics of the orientational degrees of freedom can be expressed by the Smoluchowski equation for the orientational distribution function $f(\mathbf{u}; t)$,

TABLE I. Nomenclature (selected quantities).

λ	h	M_{sat}	ϕ	χ_L	ζ_{rot}	ζ_t	τ_{rot}	κ_0	κ
$\frac{\mu_0 m^2}{4\pi\sigma^3 k_B T}$	$\frac{\mu_0 m H}{k_B T}$	nm	$\frac{\pi\sigma^3 n}{6}$	$8\lambda\phi$	$\pi\eta_s\sigma^3$	$3\pi\eta_s\sigma$	$\frac{\zeta_{\text{rot}}}{3k_B T}$	$\frac{3\tau}{5\tau_{\text{rot}}}$	$\frac{24}{7}\kappa_0$

$$\frac{\partial f}{\partial t} = -\mathcal{L} \cdot \left[\left(\boldsymbol{\Omega} - \frac{1}{\zeta_{\text{rot}}} \mathcal{L} \Phi_{\text{eff}} \right) f \right] + \frac{k_B T}{\zeta_{\text{rot}}} \mathcal{L}^2 f. \quad (11)$$

The magnetization is determined from f by $\mathbf{M} = M_{\text{sat}} \langle \mathbf{u} \rangle$, where $\langle \mathbf{u} \rangle(t) = \int d^2 u \mathbf{u} f(\mathbf{u}; t)$. In principle, the orientational and translational degrees of freedom are coupled by the dipolar interactions. For low concentrations and small λ , the combined effect of a magnetic field and dipolar interactions can be described by a local magnetic field $\mathbf{h}_{\text{loc}} = \mathbf{h} + \chi_L \langle \mathbf{u} \rangle$, with $\Phi_{\text{loc}} = -k_B T \mathbf{u} \cdot \mathbf{h}_{\text{loc}}$. In this approximation, the equilibrium magnetization is given by $M_{\text{eq}} = M_{\text{sat}} L_1(h_{\text{loc}})$, where $L_1(x) = \coth(x) - x^{-1}$ is the Langevin function. In the presence of a flow field $\mathbf{v}(\mathbf{r})$ with a symmetric velocity gradient \mathbf{D} , the dipolar interactions are modified via the flow-induced distortion of the pair correlation function. This effect was taken into account in Ref. [7] within a Kirkwood-Smoluchowski equation. For weak, time-independent flows, this effect can be approximated by an additional contribution to the effective potential,

$$\frac{\Phi_{\text{eff}}}{k_B T} = -\mathbf{u} \cdot \mathbf{h}_{\text{loc}} + \frac{6}{5} \chi_L \tau \mathbf{u} \cdot \mathbf{D} \cdot \langle \mathbf{u} \rangle. \quad (12)$$

In Eq. (12), we have introduced the translational relaxation time τ , which enters the Kirkwood-Smoluchowski equation as an additional parameter [7].

Inserting the effective potential Eq. (12) into the kinetic equation (11) defines DMF model of weakly interacting magnetic dipoles proposed in [7]. In the limit $\chi_L \rightarrow 0$, the kinetic model of noninteracting magnetic dipoles (NI) is recovered as a special case. (See Table I.)

A. Nonequilibrium magnetization in mean-field approximation

The magnetization dynamics is obtained from the Smoluchowski equation (11) by multiplication with \mathbf{u} and subsequent integration over \mathbf{u} . Due to interactions, however, no closed equation for the magnetization can be obtained by this procedure. To overcome the closure problem, the so-called effective field approximation has frequently been employed in the literature [4,17]. In [17], we have shown that the effective field approximation gives very accurate predictions in the noninteracting case for weak and moderate shear rates.

Within the effective field approximation, the nonequilibrium magnetization for small shear rates $\tau_{\text{rot}} \dot{\gamma} \ll 1$ is found to be given by

$$\frac{\mathbf{M}}{M_{\text{sat}}} = \frac{\mathbf{M}_{\text{eq}}}{M_{\text{sat}}} + \tau_{\text{rot}} \dot{\gamma} \frac{3S_1^2}{h(2+S_2)} \begin{pmatrix} \hat{h}_y [1 - B(1 - 2\hat{h}_x^2)] \\ -\hat{h}_x [1 + B(1 - 2\hat{h}_y^2)] \\ 2B\hat{h}_x \hat{h}_y \hat{h}_z \end{pmatrix}, \quad (13)$$

where we have defined $B = \kappa_0 \chi_L (2 + S_2) / 3$. To first order in $\tau_{\text{rot}} \dot{\gamma}$, the orientational order parameters S_j can be replaced

by their equilibrium values $S_j(h) = L_j(h_{\text{loc}})$, where $L_1(x) = \coth(x) - x^{-1}$ is the Langevin function introduced above and $L_2(x) = 1 - 3L_1(x)/x$. The ratio of relaxation times $\kappa_0 = 3\tau / (5\tau_{\text{rot}})$ occurs in B , where $\tau_{\text{rot}} = \pi\eta_s\sigma^3 / (3k_B T)$ denotes the orientational relaxation time of a sphere with diameter σ in a solvent with viscosity η_s .

From Eq. (13) we observe that the flow induced nonequilibrium magnetization is different, if the magnetic field is oriented in the flow ($i=1: \hat{h}_x=1, \hat{h}_y=\hat{h}_z=0$) or in the gradient ($i=2: \hat{h}_y=1, \hat{h}_x=\hat{h}_z=0$) direction. In the noninteracting case, $\chi_L \rightarrow 0$, the absolute values of the magnetization components become equal. Thus if we define an average nonequilibrium magnetization by $2M^\perp = M_y(i=1) + M_x(i=2)$, the DMF model predicts (i) that the non-equilibrium magnetization components are related, $M^\perp = \frac{1}{2} [M_x(i=4) - M_{\text{eq}}]$, where $M_x(i=4)$ denotes the magnetization in case the magnetic field is oriented along the bisector of the flow and gradient direction, and (ii) that $(h/S_1^\perp) M^\perp = \text{const}$, i.e. independent of h . The value of this constant is a direct measure for the strength of dipolar interactions.

B. Viscosity coefficients in mean-field approximation

For spatially homogeneous systems, the symmetric contribution to the viscous pressure tensor (9) can be reexpressed in terms of the pair correlation function. Employing a Kirkwood-Smoluchowski equation for the pair correlation function [7,18], the viscous pressure tensor becomes [7]

$$\mathbf{P} = p\mathbf{1} - 2\tilde{\eta}_0 \mathbf{D} - 7a \overline{\langle \mathbf{u} \rangle \langle \mathbf{u} \rangle} \times \boldsymbol{\Omega} - 2a(c_1 - 3) \overline{\mathbf{D} \cdot \langle \mathbf{u} \rangle \langle \mathbf{u} \rangle} + \frac{1}{2} n k_B T \overline{\langle \mathbf{u} \rangle \mathbf{h} - \mathbf{h} \langle \mathbf{u} \rangle}. \quad (14)$$

In Eq. (14), we have introduced $a \equiv 2\eta_s \kappa \lambda \phi^2$, where $\kappa = (24/7)\kappa_0$. The shear viscosity of the isotropic suspension is $\eta_0 = \eta_s (1 + \frac{5}{2}\phi + b\phi^2)$, where $b \equiv \frac{7}{6} c_4 \kappa$ and $\tilde{\eta}_0 \equiv \eta_0 - \frac{1}{3}(c_1 - 3)a \langle \mathbf{u} \rangle^2$. The coefficients c_k depend on the detailed form of the short range interaction potential. For the WCA potential considered in Sec. II and in the limit of small concentrations where the pair correlation function of the reference fluid can be approximated by $g(r) \approx \exp[-\beta\Phi^*(r)]$ for $r > \sigma$ and zero else, these coefficients take the values $c_1 \approx 7.72$ and $c_4 \approx 8.36$. A reduced temperature of $T^* = 1$ has been assumed. For potentials with softer repulsion higher values of c_1 and c_4 are obtained.

The only parameter in the DMF model which is not specified so far is the translational relaxation time τ entering the dimensionless quantity κ . In principle, τ can be determined from molecular simulations of structural relaxation in non-magnetic systems. Here, we use as a rough estimate the time

TABLE II. Definition of reduced units and main simulation parameters.

Parameter		Reduced units
σ	(soft) particle radius	$\equiv 1$
M	particle mass	$\equiv 1$
ϵ	(separation) interaction energy	$\equiv 1$
μ_0	magnetic susceptibility	$\equiv 1$
N	number of particles	2048–10976
ϕ	volume fraction	0.02–0.16
λ	dipolar interaction parameter	0.25–2.0
T^*	temperature	1
$\dot{\gamma}^*$	shear rate	0.0–0.1

to travel a particle diameter $\tau \approx \tau_0 = (M\sigma^2/\epsilon)^{1/2}$. With this choice no adjustable parameters are left in the DMF model.

In a steady shear flow with the linear velocity profile $\mathbf{v} = (\dot{\gamma}y, 0, 0)$, the shear viscosity η_{yx} can be calculated from Eq. (14) explicitly. If the magnetic field is oriented in the flow ($i=1$), gradient ($i=2$), vorticity ($i=3$) direction or parallel to the bisector between the flow and gradient direction ($i=4$), the DMF model predicts the following viscosity coefficients

$$\eta_i = \eta_0 + \frac{3}{2} \eta_s \phi \frac{3S_1^2}{2 + S_2} \left[(1 - \delta_{i,3}) + d_i \kappa \chi_L \frac{2 + S_2}{3} \right], \quad (15)$$

where the constants d_i are defined by $d_1 = (c_1/6 + 3)/6$, $d_2 = (c_1/6 - 4)/6$, $d_3 = (1 - c_1/3)/6$, and $d_4 = -d_3$. In the theory of liquid crystals, the viscosity coefficients η_i are known as Miesowicz viscosities [13,16]. Instead of η_4 the Helfrich viscosity coefficient is frequently employed, which is defined as $\eta_{12} = 4\eta_4 - 2(\eta_1 + \eta_2)$. From Eq. (15) we find $\eta_{12} = \frac{1}{2}(c_1/3 - 1)\eta_s \phi \kappa \chi_L S_1^2$.

From Eq. (15) we find that $\eta_1 > \eta_2$. The same relation holds for a dilute suspension of oblate ellipsoids, while the opposite inequality applies in case of prolate ellipsoids [16]. In the absence of interactions, $\chi_L = 0$, the result of the noninteracting model is recovered from (15), $\eta_1 = \eta_2 = \eta_4$, $\eta_3 = \eta_0$ and $\eta_{12} = 0$. For the special case of dilute systems, $c_1 \approx 7.72$ is obtained for the WCA potential (see above). In this case, $d_1 \approx 0.71$, $d_2 \approx -0.45$, $d_3 \approx -0.26$ and the following inequalities hold $\eta_1 > \eta_4 > \eta_2$.

IV. RESULTS

A plane Couette flow $\mathbf{v} = (\dot{\gamma}y, 0, 0)$ with constant shear rate $\dot{\gamma}$ is considered exclusively in the sequel. The equations of motion (5) and (6) are integrated numerically starting from a given initial configuration with random dipole orientations. An adaptive time step of order $\Delta t/t_{\text{ref}} = 0.001$ has been employed with the reference time $t_{\text{ref}} = (M\sigma^2/\epsilon)^{1/2}$. The reduced shear rate $\dot{\gamma}^* = t_{\text{ref}}\dot{\gamma}$ was chosen as $\dot{\gamma}^* = 0.1$ if not stated otherwise. We demonstrated in [9] that this value is within the weak shear flow limit. A reduced temperature $T^* = k_B T/\epsilon = 1.0$ has been chosen in all simulations. The mag-

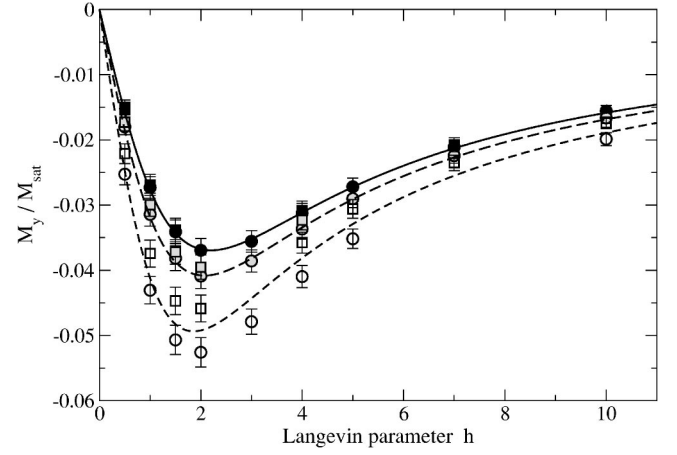


FIG. 1. The nonequilibrium magnetization M_y/M_{sat} is shown as a function of the Langevin parameter h . The magnetic field was oriented in the flow direction. Circles and squares correspond to volume fractions of $\phi=0.05$ and $\phi=0.1$, respectively. Solid, shaded, and open symbols correspond to $\chi_L=0.2$, 0.4, and 0.8, respectively. Also shown are the predictions of the DMF model, cf. Eq. (13).

netic particles are treated as rigid spheres, for which the moment of inertia tensor takes the form $\Theta = \Theta \mathbf{1}$ with $\Theta = M\sigma^2/10$. The translational friction coefficient ζ_t is chosen as $\zeta_t = 10 t_{\text{ref}}\epsilon/\sigma^2$. In order to study bulk properties in a finite, sheared system, Lees-Edwards periodic boundary conditions are employed [12]. The long range dipolar interactions are treated by the reaction field method [12]. A cavity radius $r_{\text{RF}} = 2.5\sigma$ and metallic boundary conditions have been chosen. Typically, systems with $N=2048$ and $N=10976$ particles are considered. We have demonstrated already in [9], that these values are sufficiently large to avoid finite size effects on the simulation results. We also showed in [9] that the results do not change significantly upon increasing r_{RF} . The integration is carried out for at least 10^5 time steps until a stationary state has been reached. Magnetic and viscous properties of the system are extracted as time averages for another time interval of at least 5×10^5 time steps. Error bars are estimated from block averages [12].

Volume fractions $\phi = N\pi\sigma^3/6V$ between $\phi=0.02$ and $\phi=0.16$ are considered which are typical for ferrofluids [1]. The dipolar interaction parameter (4) is chosen in the range $0.25 \leq \lambda \leq 2$. The magnetic field is oriented either in flow, gradient or in vorticity direction or parallel to the bisector of the flow and gradient direction. The main simulation parameters are collected in Table II.

A. Magnetic properties

In Fig. 1, the nonequilibrium magnetization M_y/M_{sat} is shown as a function of the Langevin parameter h . The magnetic field was oriented in the flow direction. Results for different values of the volume fraction ϕ and dipolar interaction parameter λ are shown. Also shown are the predictions of the DMF model given by Eq. (13). We observe from Fig. 1, that the nonequilibrium magnetization is well described by the dynamical mean-field theory for $\chi_L \leq 0.4$, where $\chi_L = 8\lambda\phi$ denotes the Langevin susceptibility. For

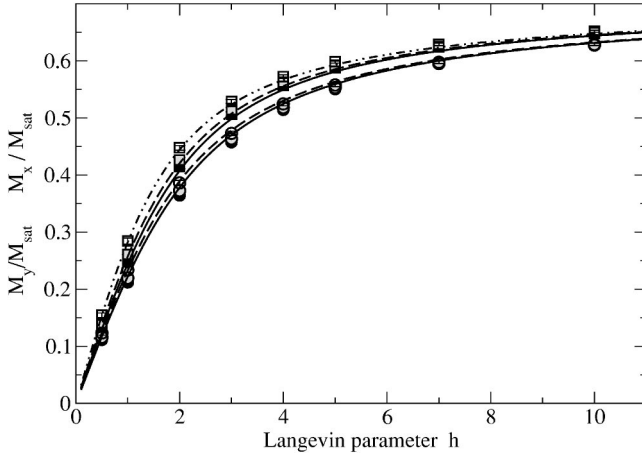


FIG. 2. The nonequilibrium magnetization components M_x/M_{sat} (circles) and M_y/M_{sat} (squares) are shown as a function of the Langevin parameter h . The magnetic field was oriented parallel to the bisector between the flow and the gradient direction. Again, solid, shaded, and open symbols correspond to $\chi_L=0.2, 0.4$, and 0.8 , respectively. Also shown are the predictions of the DMF model; cf. Eq. (13).

$\chi_L=0.8$ we observe that the absolute value of M_y is bigger for $\phi=0.05, \lambda=2.0$ than for $\phi=0.1, \lambda=1.0$. Thus, we must conclude that for $\chi_L \geq 0.8$ the DMF model is not applicable since the nonequilibrium magnetization is no longer a function of χ_L only but depends on ϕ and λ separately. The predictions of the DMF model agree well with the simulation results for weak interactions, $\chi_L \leq 0.4$.

The case when the magnetic field is oriented in the gradient direction was already considered in [9]. A similar behavior as shown in Fig. 1 has been observed for the nonequilibrium magnetization M_x , except that M_x is positive in this case; see Eq. (13).

If the magnetic field is oriented in the vorticity direction, no flow induced magnetization component in flow or gradient direction is observed within the error bars of the simulation. This observation is in agreement with the DMF model predictions.

Figure 2 shows the nonequilibrium magnetization components M_x/M_{sat} and M_y/M_{sat} if the magnetic field is oriented parallel to the bisector of the flow and gradient direction. In this case, both magnetization components are equal in equilibrium. In a planar shear flow, the magnetization component in flow direction is increased, while the component in gradient direction is decreased. Also shown are the predictions of the DMF model, Eq. (13), for $\hat{h}_x = \hat{h}_y = 1/\sqrt{2}$, and $\hat{h}_z = 0$. We find that the predictions of the DMF model accurately describe the simulation results even for $\phi=0.1$ and $\lambda=1.0$. Moreover, we observe that the simulation results for $\phi=0.1, \lambda=1.0$ agree with those for $\phi=0.05, \lambda=2.0$ (not shown) within the error bars. It seems therefore that in this geometry the Langevin susceptibility is the only control parameter for $\chi_L \leq 0.8$.

B. Viscous properties

In Fig. 3, the relative change of shear viscosity $(\eta_{yx} - \eta_0)/\eta_0$ is shown as a function of the Langevin parameter h .

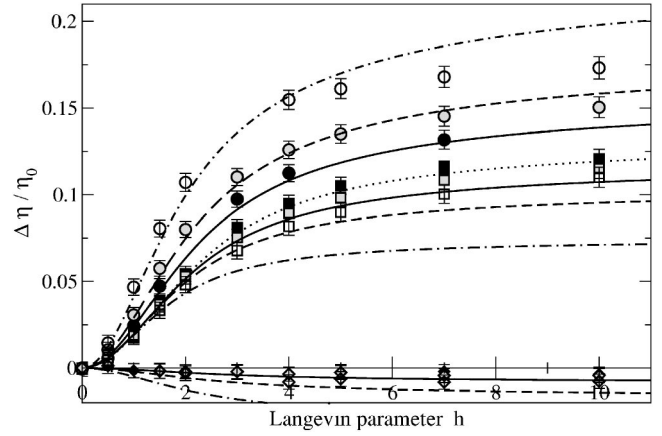


FIG. 3. The relative change of shear viscosity $\Delta\eta_{yx}/\eta_0$ is shown as a function of the Langevin parameter h . Circles, squares, and diamonds correspond to orientations of the magnetic field in the flow, gradient, and vorticity direction of the flow, respectively. The volume fraction was chosen as $\phi=0.1$. Solid, shaded, and open symbols correspond to $\lambda=0.25, 0.5$, and 1.0 , respectively. Also shown are the predictions of the DMF model; cf. Eq. (15).

Note that the shear viscosity contains contributions from the symmetric (9) and antisymmetric part (10) of the viscous pressure tensor. The magnetic field was oriented either in the flow, gradient, or in the vorticity direction. Also shown are the corresponding Miesowicz viscosities η_1, η_2 , and η_3 calculated from Eq. (15). While η_1 and η_2 increase with increasing magnetic field strength h , η_3 is found to decrease with increasing h , thereby $\eta_3 - \eta_0$ becoming negative. While the values of η_1 and η_2 are comparable, the absolute value of η_3 is significantly smaller. These observations are in agreement with the experimental results of [5]. The NI model predicts identical values for η_1 and η_2 , shown by the dotted line, while η_3 is predicted to be independent of h . For the present choice of parameters, the simulation results deviate considerably from these predictions. For a volume fraction of $\phi=0.1$ and dipolar interaction strengths $\lambda=0.25$ and 0.5 , the simulation results are accurately described by the DMF model (solid and dashed lines, respectively). For stronger dipolar interactions, $\lambda \geq 1$, the simulation results start to deviate from the predictions of the DMF model (dashed-dotted lines). A similar range of validity of the DMF model was found for the nonequilibrium magnetization. It is interesting to note that the deviations from the DMF model are stronger for η_2 and η_3 than for η_1 , which is still rather accurately described by the DMF model even for $\lambda=1$.

Figure 4 shows the relative change of shear viscosity $(\eta_{yx} - \eta_0)/\eta_0$ as a function of the volume fraction ϕ . Results for the Miesowicz viscosities η_1, η_2 , and η_3 corresponding to different orientations of the magnetic field with respect to the flow geometry are shown. Results for dipolar interaction strengths of $\lambda=0.5$ and 1.0 are shown. A strong magnetic field $h=20.0$ was employed in the simulation. Comparison to the prediction of the DMF model (dashed line), cf. Eq. (15), shows very good agreement for volume fraction $\phi \leq 0.1$. Similar to the above findings, the simulation results for η_1 and η_3 are well described up to $\phi \approx 0.15$, while stronger deviations from the DMF model are observed for η_2 . It is

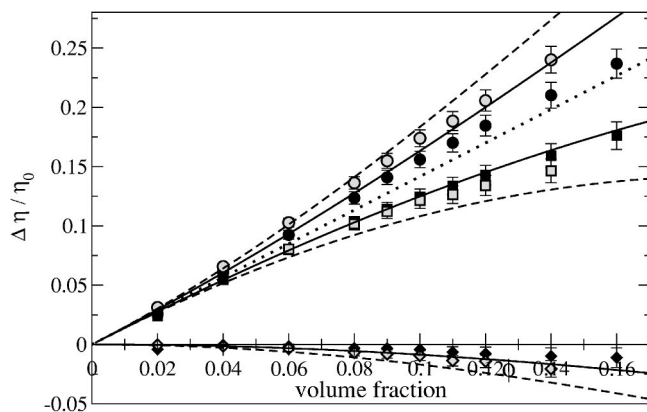


FIG. 4. The relative change of shear viscosity as a function of the volume fraction ϕ for dipolar interaction strengths $\lambda=0.5$ (full symbols) and 1.0 (open symbols). The value of the Langevin parameter was chosen as $h=20.0$. Circles, squares, and diamonds show the simulation results for magnetic fields oriented in the flow, gradient, and vorticity direction, respectively. Solid and dashed lines are the result of the DMF model for $\lambda=0.5$; dotted line the NI model.

interesting to note that the comparison between the DMF model and the simulation results can be improved if the structural relaxation time is assumed to be $\tau \approx \tau_0/2$ instead of $\tau \approx \tau_0$ (solid lines in Fig. 4), i.e., the time to travel the particle radius rather than the particle diameter. Therefore, both estimates of τ seem to be acceptable.

V. CONCLUSIONS

Extensive molecular simulations have been performed in order to investigate the anisotropy of the magnetoviscous effect. A planar, steady shear flow with the magnetic field oriented in the flow, gradient, or vorticity direction or parallel to the bisector of the flow and gradient direction has been considered. We observe that dipolar interactions lead to

different viscosity coefficients depending on the orientation of the magnetic field. The difference in the viscosity coefficients η_1 and η_2 if the magnetic field is oriented in the flow and in the gradient direction cannot be explained within the noninteracting model. In both cases, the magnetic field is perpendicular to the vorticity direction. Therefore, the difference between η_1 and η_2 gives information on the strength of particle interactions. Similarly, the viscosity coefficient η_3 that is measured if the magnetic field is oriented in the vorticity direction is identical to the zero-field viscosity in the noninteracting model. Therefore, deviations of η_3 from the zero-field viscosity also give information on particle interactions. For moderate interaction strengths, $\chi_L \leq 0.4$ the viscosity coefficients are well described by the dynamical mean-field model. For stronger interactions, the model has to be extended by including higher order terms in the dipolar interaction strength. Some steps in this direction have been proposed in [7] but the consequences for the magnetoviscous effect have not been worked out so far. For very strong dipolar interactions where permanent, chainlike aggregates are assumed, the chain model [6] has been employed in order to investigate magnetoviscous properties [16]. We hope that further experimental studies on well-characterized ferrofluids will be performed in order to further investigate the anisotropy of the magnetoviscous effect. It should be noted, however, that in experiments the external field \mathbf{H}_0 is controlled, while the present study assumes a given internal field \mathbf{H} . Both fields are related via the demagnetization coefficient and the magnetization. Thus using the results for the magnetization presented in the present study and the demagnetization coefficient appropriate for the experimental condition allows us to recalculate the external field corresponding to the internal field considered here.

ACKNOWLEDGMENTS

This work has been performed under the auspices of the DFG-SPP 1104 “Kolloidale magnetische Flüssigkeiten.”

-
- [1] *Ferrofluids. Magnetically Controllable Fluids and Their Applications*, edited by S. Odenbach, Lecture Notes in Physics Vol 594 (Springer, Berlin, 2002).
- [2] R. E. Rosensweig, *Ferrohydrodynamics* (Cambridge University Press, Cambridge, England, 1985).
- [3] J. P. McTague, *J. Chem. Phys.* **51**, 133 (1969).
- [4] M. A. Martsenyuk, Y. L. Raikher, and M. I. Shliomis, *Sov. Phys. JETP* **38**, 413 (1974).
- [5] A. Grants, A. Irbitis, G. Kronkalns, and M. M. Maiorov, *J. Magn. Magn. Mater.* **85**, 129 (1990).
- [6] A. Y. Zubarev and L. Y. Iskakova, *Phys. Rev. E* **61**, 5415 (2000).
- [7] P. Ilg and S. Hess, *Z. Naturforsch., A: Phys. Sci.* **58**, 589 (2003).
- [8] S. Odenbach and H. W. Müller, *Phys. Rev. Lett.* **89**, 037202 (2002).
- [9] P. Ilg, M. Kröger, and S. Hess, *Phys. Rev. E* **71**, 031205 (2005).
- [10] Z. Wang, C. Holm, and H. W. Müller, *Phys. Rev. E* **66**, 021405 (2002).
- [11] H. Morimoto and T. Maekawa, *Int. J. Mod. Phys. B* **15**, 823 (2001).
- [12] M. P. Allen and D. J. Tildesley, *Computer Simulation of Liquids* (Oxford University Press, Oxford, 1987).
- [13] M. Kröger, P. Ilg, and S. Hess, *J. Phys.: Condens. Matter* **15**, S1403 (2003).
- [14] B. U. Felderhof, *Phys. Rev. E* **62**, 3848 (2000).
- [15] H. Kelker and R. Hatz, *Handbook of Liquid Crystals* (Verlag Chemie, Weinheim, 1980).
- [16] P. Ilg and M. Kröger, *Phys. Rev. E* **66**, 021501 (2002); **67**, 049901(E) (2003).
- [17] P. Ilg, M. Kröger, and S. Hess, *J. Chem. Phys.* **116**, 9078 (2002).
- [18] S. Hess, *Phys. Rev. A* **22**, 2844 (1980).